JOURNAL OF SOLID STATE CHEMISTRY 31, 59–67 (1980)

The Crystal Structure and Some Properties of Eu_2Sb_3

G. CHAPUIS,* F. HULLIGER,† AND R. SCHMELCZER*

**Institut de Cristallographie de l'Université de Lausanne, CH-1015 Lausanne-Dorigny; †Laboratorium für Festkörperphysik ETH, CH-8093 Zürich, Switzerland*

Received January 22, 1979; in final form April 26, 1979

The Mooser–Pearson phase Eu_2Sb_3 crystallizes in a new monoclinic structure type, space group $P2_1/c$ (No. 14) with $a = 6.570(1)$ Å, $b = 12.760(2)$ Å, $c = 15.028(2)$ Å, $\beta = 90.04(1)°$; $Z = 8$. The Sb atoms form six-membered twisted chain fragments oriented along the b-axis. The Eu atoms are eight- and nine-coordinated by Sb. The Eu_2Sb_3 structure is closely related to the structure of Ca_2As_3. The relations between their space-group symmetries are derived and hypothetical higher-symmetry structures are discussed. The semiconducting Eu_2Sb_3 is antiferromagnetic below $T_N = 14.4$°K. An Eu_2Sb_3-type structure was found also for Sr_2Sb_3.

Introduction

In the last two decades the investigations of the rare-earth pnictides concentrated mainly on the rock salt-type compounds. The study of other phases was largely neglected and in fact phase diagrams are known only in some rare cases. The europium pnictides particularly did not attract much attention because the known NaCl-type phases EuN and EuP contain the cation in the trivalent state and therefore show no magnetic ordering at low temperatures, in contrast to the well-studied Eu monochalcogenides. Only recently, efforts have been made to investigate the various pnictide phases of Eu and Yb (*1*), the crystal chemistry of which resembles that of the alkaline-earth pnictides more closely than that of the remaining pnictides.

On preparing $EuSb_2$ crystals (*2*) we also obtained some darker crystals of which the composition, according to an electron-beam microanalysis, was $Eu_{39.9}Sb_{60.1\pm0.2}$.

These crystals were used for the structure determination described in this paper. Meanwhile the crystal structure of Eu_2Sb_3 has been mentioned by Taylor *et al.* (*1*) to be of the Ca_2As_3 type (*3*) which was found also in Eu_2As_3 (*1*). Guinier patterns indeed appeared to confirm this assignment. Our structure determination on single crystals, however, led to a different though closely related structure for Eu_2Sb_3. Possibly Eu_2Sb_3 occurs in two modifications, both being nonmetallic.

Structure Determination

The single crystal chosen for the structure determination had an irregular trigonal-prismatic shape with approximate dimensions of $0.08 \times 0.08 \times 0.05$ mm. Precession patterns showed the symmetry to be monoclinic and the systematic extinctions ($h0l$), $l = 2n + 1$, and ($0k0$), $k = 2n + 1$, leading to the space group $P2_1/c$ (No. 14). Diffraction data for the structure determination were

0022-4596/80/010059-09$02.00/0

collected on a SYNTEX $P2_1$ automatic four-circle diffractometer with Nb-filtered Mo$K\alpha$ radiation ($\lambda_{MoK\bar{\alpha}} = 0.71069$ Å). The lattice constants, as given in Table I, were calculated by a least-squares procedure using 24 accurately centered reflections in the range $45° \leq 2\theta \leq 55°$. In this range the separation of $K\alpha_1$ and $K\alpha_2$ lines allowed the centering of the reflections on $K\alpha_1$ ($\lambda = 0.70926$ Å). The intensities were measured by the θ–2θ scan method and the background was evaluated from the scan profile (*4, 5*). A complete set of data ($+h, +k, \pm l$) was collected up to $(\sin\theta/\lambda)_{max} = 0.74$. The intensities were corrected for absorption ($\mu_{MoK\alpha} = 324\ cm^{-1}$) by the Gaussian integration method yielding transmission factors between 0.27 and 0.39. The reduction of the data resulted in 3943 independent intensities of which 2414 were larger than $3\sigma(I)$. The structure was solved by direct methods using the program MULTAN (*6*). For all other calculations the programs of the X-Ray System 72 (*7*) were used. Scattering factors for the neutral atoms Eu^0 and Sb^0 were taken from Cromer and Mann (*8*), the anomalous dispersion factors from Cromer (*9*). The structure was refined by full-matrix least squares, minimizing the quantity $\sum w(|F_o| - |F_c|)^2$. The weights were taken as $\{\sigma(|F_o|)\}^{-2}$. The positional and anisotropic thermal parameters are listed in Table I. The R values obtained were $R = \sum |\Delta F| / \sum |F_o| = 0.064$ and weighted $R_w = 0.069$. A final difference Fourier map showed mainly peaks in the vicinity of the atoms, resulting probably from series termination effects.[1]

Characteristic features of this structure are weak reflections with indices $k = 2n+1$ (all hkl), $k/2 + l = 2n+1$ ($0kl$, k even), and $h + k/2 = 2n+1$ ($hk0$, k even). The major part of the unobserved intensities defined by $I < 3\sigma(I)$ (38% of all reflections) belongs to these groups. This implies that the structure of Eu_2Sb_3 must be a slightly deformed version of a structure with higher symmetry of which the b-axial length is half that of the real structure. The space-group symmetry of this subcell is *Pncn* (No. 52). The R value of the main reflections ($k = 2n$) is 0.027, while the R value of the difference reflections ($k = 2n+1$) is 0.17. This relatively high value is due to the lower accuracy of the weak intensities. The values of the anisotropic thermal coefficients are very low and show a nearly isotropic and equal behavior of all the Eu and Sb atoms in this structure.

[1] A list of the observed structure factors can be requested from the authors in Lausanne.

TABLE I

DATA FOR THE MONOCLINIC ROOM-TEMPERATURE (295°K) CRYSTAL STRUCTURE OF Eu_2Sb_3[a]

Atom	x	y	z	U_{11}	U_{22}	U_{33}	U_{12}	U_{13}	U_{23}
Eu_I	0.0034(2)	0.2785(1)	0.2445(1)	0.0132(5)	0.0106(5)	0.0108(7)	0.0012(6)	0.0008(5)	0.0000(7)
Eu_{II}	0.5053(2)	0.4711(1)	0.2537(1)	0.0128(5)	0.0113(5)	0.0129(6)	0.0025(6)	−0.0002(5)	−0.0022(7)
Eu_{III}	0.7454(2)	0.3759(1)	0.4959(1)	0.0152(6)	0.0106(7)	0.0110(8)	−0.0042(5)	0.0022(6)	0.0000(6)
Eu_{IV}	0.2465(2)	0.3733(1)	−0.0030(1)	0.0139(6)	0.0130(6)	0.0103(7)	0.0006(5)	−0.0015(5)	−0.0008(6)
Sb_I	0.2365(3)	0.3825(2)	0.4257(1)	0.0138(8)	0.0109(9)	0.016(1)	−0.0012(7)	−0.0011(7)	0.0033(8)
Sb_{II}	0.0360(3)	0.0330(2)	0.1592(1)	0.0107(8)	0.0121(9)	0.013(1)	0.0035(7)	−0.0011(7)	−0.0023(8)
Sb_{III}	0.0842(3)	0.5439(2)	0.1554(1)	0.0115(9)	0.0142(9)	0.0115(9)	0.0041(7)	−0.0023(7)	−0.0016(8)
Sb_{IV}	0.5786(3)	0.2042(2)	0.3429(1)	0.0137(9)	0.0101(9)	0.013(1)	−0.0020(7)	0.0028(7)	−0.0026(7)
Sb_V	0.4613(3)	0.2201(2)	0.1579(1)	0.0127(8)	0.0120(9)	0.0103(9)	0.0044(7)	0.0030(7)	0.0017(7)
Sb_{VI}	0.7379(3)	0.3687(2)	0.0728(1)	0.0144(8)	0.0094(9)	0.014(1)	0.0010(7)	0.0010(7)	0.0018(8)

[a] Space group $P2_1/c$ (No. 14), $Z = 8$; all atoms in 4(*e*): $\pm(x, y, z; x, \frac{1}{2}-y, \frac{1}{2}+z)$; $a = 6.570(1)$ Å, $b = 12.760(2)$ Å, $c = 15.028(2)$ Å, $\beta = 90.04(1)°$; $\rho_{calc} = 7.06\ g/cm^3$.

The anisotropic temperature factor is defined as $\exp(-2\pi^2 \sum h_i h_j a_i^* a_j^* U_{ij})$, where h_i are the Miller indices and a_i^* reciprocal-axis lengths; U_{ij} in $Å^2$. Standard deviations of the last digits are added in parentheses.

TABLE Ia

POWDER PATTERN OF Eu_2Sb_3 FOR $CuK\alpha_1$ RADIATION

d(Å)	$h\,k\,l$	I_{calc}	I_{obs}
4.577	1 2 0	67	w
3.940	0 2 3	31	vw
3.910	1 2 $\bar{2}$	54	w
3.908	1 2 2	53	
3.757	0 0 4	63	vw
3.380	1 2 $\bar{3}$	273	ms
3.378	1 2 3	275	
3.262	1 0 $\bar{4}$	137	wm
3.260	1 0 4	134	
3.011	2 0 $\bar{2}$	685	vs
3.009	2 0 2	680	
2.936	0 4 2	1000	vs
2.905	1 2 $\bar{4}$	486	vs
2.903	1 2 4	481	
2.819	1 4 $\bar{1}$	350	s
2.819	1 4 1	372	
2.723	2 2 $\bar{2}$	84	ms
2.722	2 2 2	81	
2.719	0 2 5	338	
2.681	1 4 $\bar{2}$	94	wm
2.681	1 4 2	93	
2.524	2 2 $\bar{3}$	145	m
2.522	2 2 3	147	
2.513	1 2 $\bar{5}$	212	ms
2.512	1 2 5	211	
2.432	0 4 4	38	vvw
2.307	2 2 $\bar{4}$	31	vvw
2.305	2 2 4	35	
2.289	2 4 0	767	vs
2.198	1 2 $\bar{6}$	302	s
2.197	1 2 6	305	
2.106	0 6 1	31	vvw
2.103	3 0 $\bar{2}$	97	wm
2.102	3 0 2	94	
2.082	2 4 $\bar{3}$	42	vw
2.081	2 4 3	39	
2.052	3 2 $\bar{1}$	23	vvw
2.052	3 2 1	23	
1.997	3 2 $\bar{2}$	23	vw
1.997	3 2 2	24	
1.958	0 6 3	171	wm
1.955	2 4 $\bar{4}$	56	wm
1.954	2 4 4	54	
1.944	1 2 $\bar{7}$	110	wm
1.943	1 2 7	110	
1.814	3 2 $\bar{4}$	62	w
1.813	3 2 4	65	
1.793	3 4 $\bar{1}$	41	vw
1.793	3 4 1	38	
1.736	0 6 5	101	w

TABLE Ia—*Continued*

d(Å)	$h\,k\,l$	I_{calc}	I_{obs}
1.706	3 2 $\bar{5}$	81	w
1.705	3 2 5	83	
1.679	1 6 $\bar{5}$	77	w
1.678	1 6 5	76	
1.628	3 4 $\bar{4}$	39	vw
1.627	3 4 4	40	
1.597	3 2 $\bar{6}$	54	w
1.596	3 2 6	55	
1.595	0 8 0	23	
1.5804	2 2 $\bar{8}$	20	vvw
1.5795	2 2 8	19	
1.5689	1 2 $\bar{9}$	63	w
1.5684	1 2 9	60	
1.5418	1 8 $\bar{1}$	98	m
1.5418	1 8 1	93	
1.5351	2 6 $\bar{5}$	131	m
1.5346	2 6 5	133	
1.5109	0 6 7	60	w
1.5053	4 0 $\bar{4}$	32	vw
1.5046	4 0 4	28	
1.4911	3 2 $\bar{7}$	101	wm
1.4907	3 2 7	97	
1.4726	1 6 $\bar{7}$	92	wm
1.4723	1 6 7	89	
1.4597	3 6 $\bar{3}$	78	wm
1.4593	3 6 3	80	
1.4348	2 8 0	60	w
1.4336	4 4 $\bar{2}$	91	m
1.4333	4 4 2	85	

Description of the Eu_2Sb_3 Structure

The monoclinic, nearly orthorhombic, unit cell of Eu_2Sb_3 contains eight formula units. All the atoms are located in the general positions 4(e) of the space group $P2_1/c$, as listed in Table I. The anions form six-membered twisted chain fragments,

$$Sb_I^{2-}\text{–}Sb_{II}^{-}\text{–}Sb_{III}^{-}\text{–}Sb_{IV}^{-}\text{–}Sb_V^{-}\text{–}Sb_{VI}^{2-},$$

with Sb–Sb distances of 2.92, 2.90, 3.02, 2.89, and 2.92 Å, respectively. The indicated formal charge distribution (neglecting the partly covalent Eu–Sb bonding) suggests that the Sb–Sb distances to the end members should be larger than those within the chain fragments. Surprisingly, however, the

central distance turned out to be largest, anomalously large indeed for a single bond. We have no explanation for this fact since the nonmetallic properties (see later) require true $(Sb_6)^{8-}$ polyanions, i.e., Eu_2Sb_3 has to fulfill the Mooser–Pearson bond rule (*10, 11*). (If this Sb_{III}–Sb_{IV} distance were so large that it would no longer correspond to any covalent bonding, then such a structure would be appropriate for hypothetical Mooser–Pearson phases such as $EuLaSb_3$, $YSiAs_2$, $KSrAsSe_2$, etc.)

In a way similar to that of the anions (Sb_I^{2-}, Sb_{VI}^{2-}, and Sb_{II}^{-}, Sb_{III}^{-}, Sb_{IV}^{-}, Sb_V^{-}, respectively), the divalent cations can also be divided into two groups, namely, Eu_I, Eu_{II}, and Eu_{III}, Eu_{IV}. In Table II the Eu–Sb distances are shown up to 3.9 Å. For Eu_{III} and Eu_{IV} eight Sb neighbors are found within coordination spheres of 3.51 and 3.53 Å, respectively. The coordinations of Eu_I and Eu_{II} are more extended. Both atoms are coordinated by nine Sb neighbors within spheres of 3.87 Å. Next-nearest Sb atoms for all of the four Eu atoms are at distances larger than 4.8 Å. Similar Eu–Sb distances have been found in $EuSb_2$ (*2*).

The partial structure of the cations in Eu_2Sb_3 is virtually identical to that of the Ca_2As_3 type. As pointed out by Deller and Eisenmann (*3*), this partial structure can be described in an idealized tetragonal cell which is obtained from the monoclinic cell by the relations $2a = b$, $\beta = 90°$. Eu_I and Eu_{II} are located at the vertices of square prisms. These prisms are linked by their faces and are *A*- and *B*-centered, both by Eu_{III} and Eu_{IV}, in alternating layers along the *c*-axis. For the axial ratio $c/b = (3/2)^{1/2} = 1.22$ (for the real structure $c/b = 1.18$) an idealized partial structure is obtained that contains two kinds of sites, but all cations possess eight equidistant neighbors. (Assuming the axial ratio $c/a = 2^{-1/2} = 0.71$, the elongated prisms are compressed to cubes. This leads to two appreciably different *M*–*M* distances, namely, M_I–$M_I = M_{II}$–$M_{II} = 2^{-1/2}a$ along

TABLE II

COORDINATIONS AND INTERATOMIC DISTANCES (Å) IN Eu_2Sb_3[a]

Eu_I–1 Sb_{IV} at 3.298(3)	1 Eu_{II} at 4.095(2)
1 Sb_{VI} at 3.320(3)	1 Eu_{II} at 4.115(2)
1 Sb_V at 3.362(2)	1 Eu_{IV} at 4.225(2)
1 Sb_{II} at 3.392(2)	1 Eu_{III} at 4.325(2)
1 Sb_I at 3.394(3)	1 Eu_{III} at 4.549(2)
1 Sb_{III} at 3.400(2)	1 Eu_{IV} at 4.550(2)
1 Sb_{II} at 3.565(2)	
1 Sb_{III} at 3.680(2)	
1 Sb_V at 3.863(2)	
Eu_{II}–1 Sb_{III} at 3.270(3)	1 Eu_I at 4.095(2)
1 Sb_I at 3.330(3)	1 Eu_I at 4.115(2)
1 Sb_{IV} at 3.355(2)	1 Eu_{III} at 4.148(2)
1 Sb_{II} at 3.379(3)	1 Eu_{IV} at 4.395(2)
1 Sb_{VI} at 3.382(3)	1 Eu_{III} at 4.549(2)
1 Sb_V at 3.450(2)	1 Eu_{IV} at 4.561(2)
1 Sb_V at 3.523(2)	
1 Sb_{IV} at 3.691(2)	
1 Sb_{II} at 3.871(3)	
Eu_{III}–1 Sb_I at 3.302(3)	1 Eu_{II} at 4.148(2)
1 Sb_V at 3.304(3)	1 Eu_I at 4.325(2)
1 Sb_{II} at 3.318(3)	1 Eu_{III} at 4.521(2)
1 Sb_{VI} at 3.329(3)	1 Eu_{II} at 4.549(2)
1 Sb_{IV} at 3.360(3)	1 Eu_I at 4.549(2)
1 Sb_{II} at 3.394(3)	1 Eu_{IV} at 4.567(2)
1 Sb_I at 3.396(3)	1 Eu_{IV} at 4.578(2)
1 Sb_I at 3.506(3)	
Eu_{IV}–1 Sb_{III} at 3.329(3)	1 Eu_I at 4.225(2)
1 Sb_{IV} at 3.333(3)	1 Eu_{II} at 4.395(2)
1 Sb_{III} at 3.398(3)	1 Eu_I at 4.550(2)
1 Sb_V at 3.415(3)	1 Eu_{II} at 4.561(2)
1 Sb_{VI} at 3.423(3)	1 Eu_{III} at 4.567(2)
1 Sb_I at 3.436(3)	1 Eu_{IV} at 4.577(2)
1 Sb_{VI} at 3.456(3)	1 Eu_{II} at 4.578(2)
1 Sb_{VI} at 3.531(3)	
Sb_I–1 Eu_{III} at 3.302(3)	1 Sb_{II} at 2.918(3)
1 Eu_{II} at 3.330(3)	1 Sb_{IV} at 3.432(3)
1 Eu_I at 3.394(3)	
1 Eu_{III} at 3.396(3)	
1 Eu_{IV} at 3.436(3)	
1 Eu_{III} at 3.506(3)	
Sb_{II}–1 Eu_{III} at 3.318 (3)	1 Sb_{III} at 2.899(3)
1 Eu_{II} at 3.379(3)	1 Sb_I at 2.918(3)
1 Eu_I at 3.392(2)	
1 Eu_{III} at 3.394(3)	
1 Eu_I at 3.565(2)	
1 Eu_{II} at 3.871(3)	

TABLE II—*Continued*

Sb_{III}–1 Eu_{II} at 3.270(3)	1 Sb_{II} 2.899(3)
1 Eu_{IV} at 3.329(3)	1 Sb_{IV} at 3.016(3)
1 Eu_{IV} at 3.398(3)	1 Sb_{VI} at 3.422(3)
1 Eu_{I} at 3.400(2)	
1 Eu_{I} at 3.680(2)	
Sb_{IV}–1 Eu_{I} at 3.298(3)	1 Sb_{V} at 2.890(3)
1 Eu_{IV} at 3.333(3)	1 Sb_{III} at 3.016(3)
1 Eu_{II} at 3.355(2)	1 Sb_{I} at 3.432(3)
1 Eu_{III} at 3.360(3)	
1 Eu_{II} at 3.691(2)	
Sb_{V}–1 Eu_{III} at 3.304(3)	1 Sb_{IV} at 2.890(3)
1 Eu_{I} at 3.362(2)	1 Sb_{VI} at 2.923(3)
1 Eu_{IV} at 3.415(3)	
1 Eu_{II} at 3.450(2)	
1 Eu_{II} at 3.523(2)	
1 Eu_{I} at 3.863(3)	
Sb_{VI}–1 Eu_{I} at 3.320(3)	1 Sb_{V} at 2.923(3)
1 Eu_{III} at 3.329(3)	1 Sb_{III} at 3.422(3)
1 Eu_{II} at 3.382(3)	
1 Eu_{IV} at 3.423(3)	
1 Eu_{IV} at 3.456(3)	
1 Eu_{IV} at 3.531(3)	

The Sb–Sb–Sb angles within the six-membered chain fragments are:

Sb_{I}–Sb_{II}–Sb_{III}: 106.52(8)°

Sb_{II}–Sb_{III}–Sb_{IV}: 103.00(8)°

Sb_{III}–Sb_{IV}–Sb_{V}: 104.53(8)°

Sb_{IV}–Sb_{V}–Sb_{VI}: 107.51(8)°

[a] Standard deviations are added in parentheses.

the cube edge and M_I–$M_{II} = a/2$ along the cube diagonal.) The displacements of the Eu_I and Eu_{II} atoms in the real structure lead to Eu–Eu distances of different lengths. Thus the shortest Eu–Eu contacts occur between Eu_I and Eu_{II} in zigzag chains along the *a*-axis. These contacts correspond to the *M*–*M* distance along the edge of the prism basis in the idealized partial structure. Only the third-closest cation–cation contact, Eu_{II}–Eu_{III} = 4.15 Å, represents a distance between cations in different sites of the idealized structure.

Geometrical Relationships

As mentioned above, small displacements (of the order of 0.1–0.2 Å) mainly of the anions lead to an orthorhombic structure, space group *Pncn* (No. 52), with $a_{orth} = a_{mon}$, $b_{orth} = \frac{1}{2}b_{mon}$, $c_{orth} = c_{mon}$, $Z = 4$, and

M_I in 4(*d*): $\pm(\frac{1}{2}, y, \frac{3}{4}; 0, \frac{1}{2}+y, \frac{1}{4})$,

M_{II} and X_I in 4(*c*): $\pm(\frac{1}{4}, \frac{1}{4}, z; \frac{1}{4}, \frac{3}{4}, \frac{1}{2}+z)$,

X_{II} in 8(*e*):

$$\pm(x, y, z; x, \bar{y}, \tfrac{1}{2}+z; \tfrac{1}{2}-x, \tfrac{1}{2}+y, \tfrac{1}{2}+z;$$
$$\tfrac{1}{2}+x, \tfrac{1}{2}+y, \bar{z}).$$

M_I and M_{II} correspond to Eu_I, Eu_{II}, and Eu_{III}, Eu_{IV}, respectively, in the monoclinic structure. X_I corresponds to Sb_I, Sb_{VI}, and X_{II} to Sb_{II}, Sb_{III}, Sb_{IV}, Sb_V. The coordinates for Eu_2Sb_3, obtained from the main reflections, are: $y(M_I) = 0.06$; $z(M_{II}) = 0.50$; $z(X_I) = 0.93$; $x(X_{II}) = 0.06$, $y(X_{II}) = 0.08$, $z(X_{II}) = 0.16$. This (hypothetical) structure contains infinite anion spiral chains X_{II}–X_{II}–X_I–X_{II}–X_{II} along the *a*-axis with one short and two longer distances: X_{II}–X_{II} = 2.9 Å and X_I–X_{II} = 3.2 Å in our example.

The orthorhombic structure can be regarded as the parent structure of both the Ca_2As_3 and the Eu_2Sb_3 types. The infinite anion spiral chains are obtained starting with the Eu_2Sb_3 structure by breaking the Sb_{III}–Sb_{IV} bonds and linking Sb_{III} by the nearest Sb_{VI} atom and Sb_{IV} with the nearest Sb_I atom. Starting with the Ca_2As_3 structure, the infinite anion spiral chains are created by linking the four-membered with the modified eight-membered chain fragments. The relationships among these three structures are visualized in Fig. 1. Table III shows the relations among their space-group symmetries. Minor variations of the anion coordinates allow one to construct spiral chains with equal *X*–*X* distances.

We ignore whether this parent structure is realized in nature, but if so, it would be appropriate for nonmetallic representatives,

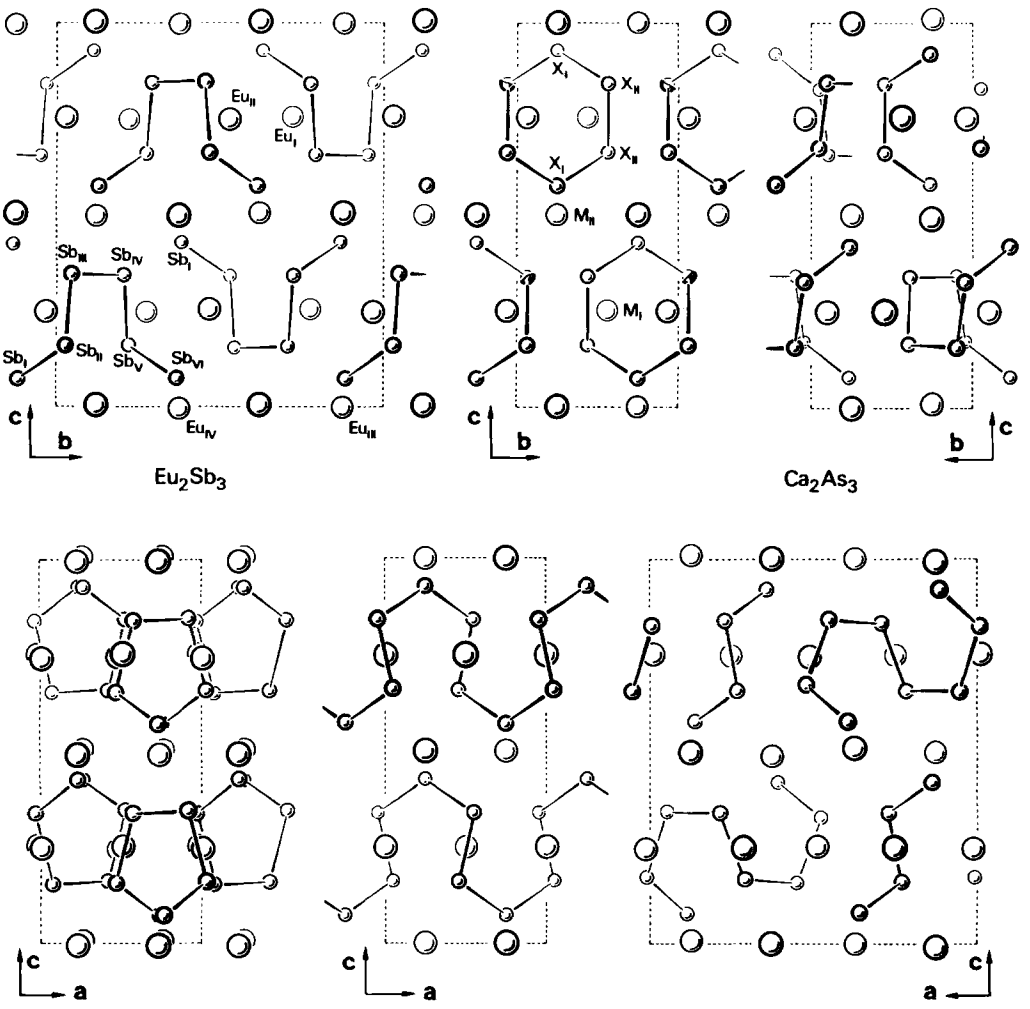

FIG. 1. Comparison of the Eu_2Sb_3 structure (left) and the Ca_2As_3 structure (right) with the hypothetical orthorhombic chain structure (middle). For Ca_2As_3 we have chosen the nearly orthorhombic cell ($P2/n$) and in the (b, c) projection (upper right corner) only the upper half of the cell is reproduced. For a strict correspondence the origin of the Ca_2As_3 cell has to be shifted by $+\frac{1}{4}$ of its a-axis and $\frac{1}{2}$ of its b-axis. Large spheres, cations; small spheres, anions.

i.e., Mooser–Pearson phases, of the kind Na_2P_2S, $BaLaSi_2As$, or (with equal X–X distances) $RbSrSb_3$, etc. If in this orthorhombic chain structure the anion spirals are additionally linked by bonds corresponding to the Sb_{III}–Sb_{IV} bonds of the Eu_2Sb_3 structure we obtain a possible structure for Mooser–Pearson phases of the kind $M_2X^{-(x-2)}X_2'^{-(x'-3)}$ (χ = anion valence, $\chi - 2$, $\chi' - 3$ = apparent anion valences with respect to the cations) such as hypothetical K_2SiAs_2 or Ca_2Si_3.

By increasing in the parent orthorhombic chain structure the X–X distance to a nonbonding value, an "impure" polyanionic phase $M_2X(X_2')$ results, adequate possibly for Mooser–Pearson phases such as Ba_2SeTe_2, $RbBaBrSe_2$, or La_2Sb_2Te. The necessary distortions may leave the space group unchanged or may increase the sym-

TABLE III

GROUP-SUBGROUP DIAGRAM SHOWING THE RELATIONS BETWEEN THE STRUCTURES OF Eu_2Sb_3 AND Ca_2As_3[a]

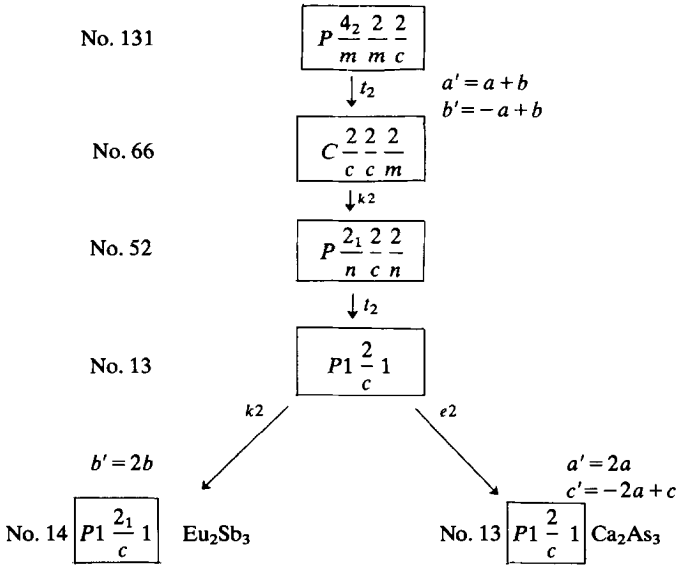

[a] Each subgroup is characterized by a letter followed by the index of the corresponding subgroup: *t* (translationsgleich) indicates a subgroup with the same cell, *k* (klassengleich) a subgroup with the same crystal class, and *e* a special case of *k* when the space group remains unchanged.

metry. By increasing the symmetry the Eu_2Sb_3 structure can finally be transformed into a tetragonal structure consisting of NaCl-type square nets and CaC_2-type layers. This idealization requires some substantial displacements. Thus we have to separate the Sb_I and Sb_{VI} atoms from the chain fragments and shift them upward or downward into the (Eu_{III}, Eu_{IV}) planes at $z=0$ and $z=\frac{1}{2}$. Moreover, all Sb_{III}–Sb_{IV} bonds have to be eliminated by increasing the Sb_{III}–Sb_{IV} distance. The positional parameters in the original Eu_2Sb_3 cell (where now $\beta=90°$, $b/a=2$, $c/a>2$) become then

$$Eu_I \rightarrow M_I{:}0, \tfrac{1}{4}, \tfrac{1}{4};$$
$$Sb_{II} \rightarrow X_{II}{:}\ 0, 0, z;$$
$$Sb_{IV} \rightarrow X_{IV}{:}\ \tfrac{1}{2}, \tfrac{1}{4}, \tfrac{1}{2}-z;$$
$$Eu_{II} \rightarrow M_{II}{:}\ \tfrac{1}{2}, \tfrac{1}{2}, \tfrac{1}{4};$$
$$Sb_{III} \rightarrow X_{III}{:}\ 0, 0, \tfrac{1}{2}-z;$$
$$Sb_V \rightarrow X_V{:}\ \tfrac{1}{2}, \tfrac{1}{4}, z;$$

for the CaC_2-type layer (where $z=\frac{1}{4}-r_X/c$, $2r_X=X_{II}-X_{III}=X_{IV}-X_V=$ anion bond distance) and

$$Eu_{III} \rightarrow M_{III}{:}\ \tfrac{3}{4}, \tfrac{3}{8}, \tfrac{1}{2};$$
$$Sb_I \rightarrow X_I{:}\ \tfrac{1}{4}, \tfrac{3}{8}, \tfrac{1}{2};$$
$$Eu_{IV} \rightarrow M_{IV}{:}\ \tfrac{1}{4}, \tfrac{3}{8}, 0;$$
$$Sb_{VI} \rightarrow X_{VI}{:}\ \tfrac{3}{4}, \tfrac{3}{8}, 0;$$

for the NaCl-type square net. The space group is now $P4_2/mmc$ (No. 131), a supergroup of the parent orthorhombic space group *Pncn*, but with half the unit cell (see Table III). The stacking sequence along the *c*-axis is *ABA'BA* (*A*, NaCl-type square net at $z=0$; *A'*, NaCl-type square net at $z=\frac{1}{2}$, displaced by $a/2$ with respect to *A*; *B*, CaC_2-type layer). This means that the stacking of the NaCl-type square nets (*A*, *A'*) is the same as in the rock salt structure, whereas only one kind of CaC_2-type layer (*B*) is intercalated. Such an idealized structure will hardly be

realized in Mooser–Pearson phases because the still rather close X–X' contacts between anions of adjacent layers and square nets would give rise to distortions lowering the symmetry. These deformations can be avoided, e.g., as in the $ThCr_2Si_2$ type (space group $I4/mmm$, No. 139), where $ThSi_2$ is placed into the CaC_2-type layers and Cr_2, i.e., only "cations", into the NaCl-type square nets. If the CaC_2-type layers have the composition $TeNd_2$ (anti-CaC_2 type) where, however, no Nd–Nd bonds exist, and the NaCl-type square nets are substituted by oxygen square nets, we end up with the tetragonal Nd_2O_2Te structure adequate for normal valence compounds.

Starting either from the original Eu_2Sb_3 structure or from the idealized tetragonal model structure, we can create another hypothetical "impure" polyanionic structure, one which contains anion squares. The squares are formed with Sb_{II}, Sb_{III}, Sb_{IV}, Sb_V of one chain fragment of the Eu_2Sb_3 structure and the anions of the CaC_2-type layer have then to occupy the following positions in the Eu_2Sb_3-like cell with $2a = b$, $\beta = 90°$:

$Sb_{II} \rightarrow X_{II}$: x, y, z;

$Sb_{III} \rightarrow X_{III}$: $x, y, \frac{1}{2}-z$;

$Sb_{IV} \rightarrow X_{IV}$: $\frac{1}{2}-x, \frac{1}{4}-y, \frac{1}{2}-z$;

$Sb_V \rightarrow X_V$: $\frac{1}{2}-x, \frac{1}{4}-y, z$

(with $1-x = 2y = \frac{1}{4}-2^{-1/2}r_X/a$, $z = \frac{1}{4}-r_X/c$; $2r_X$ is the X–X pair-bond distance).

The space group of this structure is still $P2_1/c$. Another modification is obtained by combining the X_2 pairs in such a way that the resulting squares become all parallel (X_2 pairs from the same chain fragments alternating with X_2 pairs from different chain fragments of the Eu_2Sb_3 structure). This hypothetical structure shows again short nonbonding X–X' contacts, and its formation will be more probable with a square net of small cations at the place of the NaCl-type square net. Such a substitution, however, changes the M_2X_3 phase into a true polyanionic ternary phase, $MM'_2X_2^{-(x-2)}$. Mooser–Pearson phases, i.e., nonmetallic representatives, could be of the type Li_2CaSi_2.

Physical Properties of Eu_2Sb_3

The divalent oxidation state of europium, suggested by the chemical analogy between Eu_2Sb_3 and Ca_2As_3, was confirmed by the magnetic measurements. The susceptibility of Eu_2Sb_3 obeys a Curie–Weiss law corresponding to the seven $4f$ electrons of Eu^{2+}, with a paramagnetic Curie temperature $\theta_p = -10°K$. Antiferromagnetic ordering sets in at $T_N = 14.4°K$. The shift of the susceptibility-peak temperature by application of an external magnetic field is rather pronounced (Fig. 2). The magnetic susceptibility in the ordered temperature range shows very low anisotropy, switching to $\chi_\perp$ at fields below 100 Oe. At 1.5°K an effective field of about 140 kOe is sufficient to align the magnetic moments.

Superexchange coupling will be mediated mainly by Sb_I and Sb_{VI} which contribute two valence electrons to the Eu–Sb bonding. The Eu_{III} and Eu_{IV} atoms in the puckered NaCl-like "square nets" are coupled to each other by four Sb_I, Sb_{VI} neighbors, whereas the Eu_I and Eu_{II} atoms appear to be only weakly coupled by one Sb_I and one Sb_{VI} atom to the adjacent Eu_{III}, Eu_{IV} layers. On the other hand the closest direct Eu–Eu contacts occur in the (Eu_I, Eu_{II}) plane along the zigzag chains parallel to the a-axis. Probably ferromagnetic (a, b) planes are coupled antiferromagnetically in c-direction.

All our samples showed nonmetallic behavior near room temperature. A Seebeck coefficient of 90 to 100 $\mu V/°K$ was observed, with a sign corresponding to p-type conduction. From the temperature dependence of the resistivity up to 300°C we deduce an energy gap $\Delta E \geq 0.5$ eV. Resistivities

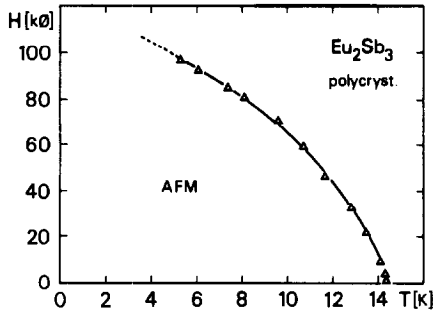

FIG. 2. Partial magnetic diagram of Eu_2Sb_3 derived from the field dependence of the susceptibility-peak temperature. The applied fields are corrected for demagnetization.

between 0.1 and 1 Ω-cm were measured at room temperature.

As was to be expected the resistivity of the isomorphous strontium analog Sr_2Sb_3 was much higher, 800 to 1000 Ω cm at 300°K. Its Seebeck coefficient turned out to be also about 100 μV/°K, but indicated *n*-type conduction.

Acknowledgments

The authors are indebted to Professor D. Schwarzenbach for helpful discussions. This study was supported by the Swiss National Science Foundation.

References

1. J. B. TAYLOR, L. D. CALVERT, T. UTSUNOMIYA, Y. WANG, AND J. G. DESPAULT, *J. Less Common Metals* **57**, 39 (1978).
2. F. HULLIGER AND R. SCHMELCZER, *J. Solid State Chem.* **26**, 389 (1978).
3. K. DELLER AND B. EISENMANN, *Z. Naturforsch. B* **31**, 1023 (1976).
4. H. BLESSING, P. COPPENS, AND D. BECKER, *J. Appl. Crystallogr.* **7**, 488 (1972).
5. D. SCHWARZENBACH, "Collected Abstracts 4th Europ. Crystallogr. Meeting, Oxford 1977," P I.20.
6. "MULTAN 76," A system of computer programs, P. Main, L. Lessinger, and M. M. Woolfson, York, England, and G. Germain and G. -P. Declerc, Louvain-la-Neuve, Belgium (1976).
7. "The X-Ray System 72," Technical Report TR-192, Computer Science Center, University of Maryland, College Park (1972); implemented and extended by D. Schwarzenbach.
8. D. CROMER AND J. MANN, *Acta Crystallogr. Sect. A* **24**, 321 (1968).
9. D. CROMER, *Acta Crystallogr.* **18**, 17 (1965).
10. E. MOOSER AND W. B. PEARSON, *Phys. Rev.* **101**, 1608 (1956); *Progr. Semicond.* **5**, 103 (1960).
11. F. HULLIGER AND E. MOOSER, *Progr. Solid State Chem.* **2**, 330 (1965).